Nonlinear passive control of a pendulum submitted to base excitations

Gabriel Hurel, Alireza Ture Savadkoohi, Claude-Henri Lamarque

Nonlinear passive control of a pendulum submitted to base excitations

G. Hurel, A. Ture Savadkoohi, C.-H. Lamarque
Univ. Lyon, ENTPE, LTDS UMR 5513,
rue Maurice Audin, 69518 Vaulx-en-Velin
Email: gabriel.hurel@entpe.fr

Published on February 22, 2021

Abstract

We seek to understand the behavior of a pendulum under parametric excitation coupled with a nonlinear absorber. First, the reference system without any coupled absorber, i.e., a simple pendulum, is analyzed with a multiple scale method thanks to supposed assumptions about the excitation. The equilibrium points of the system are calculated, and their stability is determined. The phase portraits are introduced in order to better predict the behavior of the system. Then the same analysis is performed on the pendulum coupled with the nonlinear absorber leading to detection of the slow invariant manifold and its dynamic characteristic points. Both systems are compared to estimate the effects of the absorber on the vibratory behaviors of the pendulum.

1 Introduction

Due to a variety of source of excitation such as nature (wind, earthquakes), equipment (in machines), structural interactions (cables and cabin), mechanical structures are subject to vibrations. If these vibrations are not controlled, they can lead the structure to malfunction. In the case of transportation, before the abnormal behavior and possible destruction of the structure, the vibration can induce discomfort for passengers. Many solutions have been proposed for passive control of vibration. Among the passive devices, the widely used one is the tuned mass damper [1, 2], a spring mass system able to reduce the energy of one mode of the structure. Some of these devices have been applied on passive control problem of a pendulum [3–5].
Roberson [6] showed that via introducing a nonlinearity to the restoring forcing function (cubic in this study), the absorption width of the controller would increase. Since then, many nonlinear devices have been designed [7–18]. In the nonlinear energy sink (NES) [19–24], the restoring force function is purely nonlinear, i.e. there is no linear term. This allows to broaden the range of frequency where the device is efficient as the absorber can enter to resonance with any frequency.
The passive control of the pendulum under a generalized external excitation is already studied [25, 26]. Our paper is interested in nonlinear passive control of pendular movements of a system under base excitation. Parametrically- or based-excited pendulums can behave in different manners according to the characteristics of excitations and the pendulum: Leven and Koch spotted chaotic behaviors on a damped base excited pendulum [27]. The behavior of a double pendulum under a base excitation experiences parametric excitation is studied by Sartorelli and Lacarbonara [28]. Miles [29] investigated on two nonlinear coupled pendulums presenting internal resonances under parametric excitation. Manevitch et al. [30] and Kovaleva et al [31] used the concept of limiting phase trajectories [32] for detecting behaviors of a pendulum. Meanwhile, the multiple scale methods [33] is exploited as well to study behaviors of a base-excited spring pendulums (e.g. see [34–37]). There are some works which are investigated on behaviors of double pendulums with different applications, such as biomechanics. As an example,

we can mention, modeling locomotion of human arm [38] and its passive control due to some diseases [39]. Some works are devoted to study triple pendulums which can have applications in lots to mechanical components and systems such as piston-connecting rod system[40–42]. Furthermore, there have been some works which used pendulum systems for the aim passive control: for instance, Sevin [7] studied vibrations of a undamped pendulum type vibration absorber. The behavior of a parametrically excited pendulum used as an absorber has been considered and studied with a harmonic balance method by Song et al [17]. Ikeda investigates on the passive control of a single-dof system by two pendulum tuned mass dampers [43].
In this article, we consider a pendulum with vertical and horizontal base excitations. We study the reference system in Sect. 2. Then, in Sect. 3, the pendulum is coupled to a NES. We compare both system in Sect. 4 to determine the benefit of the presence of the absorber. Finally, the paper is concluded in Sect. 5.

2 The reference system: the pendulum

2.1 Mechanical system

A planar pendulum of mass M stands in a gravitational field $\vec{g}$. It rotates around its center P with an angle θ as shown in Fig. 1. Its inertia is given by J, and its center of mass G is located at distance L from the point P. The damping coefficient of the cylindrical joint is C_θ.

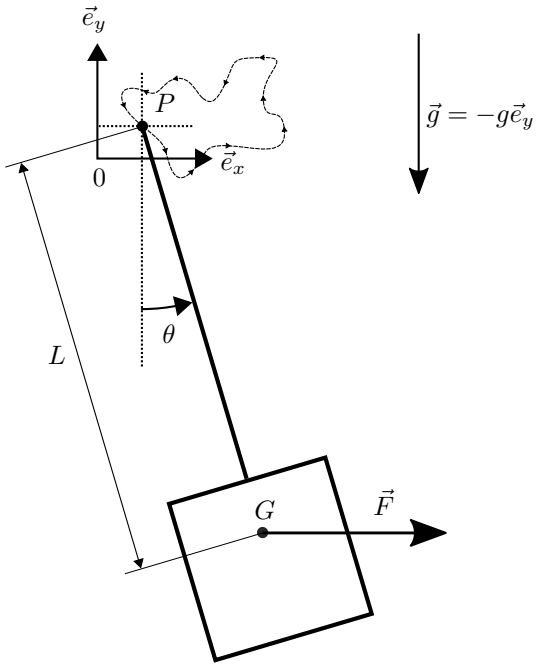

Figure 1: The pendulum in a gravity field $\vec{g}$ excited by a force $\vec{F}$ and the displacement at its base point P.

2.2 The excitation

The pendulum is subjected to a base excitation: the point P follows a imposed displacement which can be projected on directions $\vec{e}_x$ and $\vec{e}_y$ to give , respectively, $X_P(t)$ and $Y_P(t)$. We consider also a horizontal force proportional to the apparent surface of the pendulum and representing by an equivalent force F applied to the center of mass G.

$$\vec{F} = F\cos(\theta)\vec{e}_x \tag{1}$$

2.3 Governing system equations

The coordinates of the center of mass G of the pendulum read:

$$\begin{cases} x_G = X_P + L\sin(\theta) \\ y_G = Y_P - L\cos(\theta) \end{cases} \tag{2}$$

The kinetic $\mathcal{K}_r$ and potential $\mathcal{U}_r$ energies of the reference system read:

$$\mathcal{K}_r = \frac{1}{2}J\dot{\theta}^2 + \frac{1}{2}M\left(\dot{x}_G^2 + \dot{y}_G^2\right) \tag{3}$$

$$\mathcal{U}_r = Mgy_G \tag{4}$$

where $\dot{}$ refers to the derivation with respect to time t. The nonconservative forces of the system are the damping and the external forces, which read:

$$F_\theta = -C_\theta\dot{\theta} + FL\cos(\theta) \tag{5}$$

Thanks to the Lagrange equations, we can write the equation of the system:

$$\frac{\mathrm{d}^2\theta}{\mathrm{d}\tau^2} + c_\theta\frac{\mathrm{d}\theta}{\mathrm{d}\tau} + \sin(\theta) + \cos(\theta)\frac{\mathrm{d}^2x_P}{\mathrm{d}\tau^2} + \sin(\theta)\frac{\mathrm{d}^2y_P}{\mathrm{d}\tau^2} = f\cos(\theta) \tag{6}$$

where $\tau = \Omega_0 t$, $\Omega_0 = \sqrt{\dfrac{g}{L+j}}$, $j = \dfrac{J}{ML}$, $c_\theta = \dfrac{C_\theta}{\Omega_0 ML(L+j)}$, $x_P = \dfrac{X_P}{L+j}$, $y_P = \dfrac{Y_P}{L+j}$ and $f = \dfrac{F}{\Omega_0^2 M(L+j)}$.

2.4 Treatment of system equations

In order to perform a multiple scale analysis we define the small parameter $0 < \varepsilon \ll 1$ to order the terms of the equation 6. We assume that the angle θ, the excitation and the damping are small:

$$\theta = \sqrt{\varepsilon}\underline{\theta} \tag{7}$$

$$c_\theta = \varepsilon\underline{c}_\theta \tag{8}$$

$$x_P = \varepsilon^{3/2}\underline{x}_P \tag{9}$$

$$y_P = \varepsilon\underline{y}_P \tag{10}$$

$$f = \varepsilon^{3/2}\underline{f} \tag{11}$$

Furthermore, we assume that the excitation has a periodic nature. We can decompose it in the form of the Fourier series as:

$$\underline{x}_P(t) = \sum_{n=-\infty}^{\infty} x_n \mathrm{e}^{in\Omega t} \tag{12}$$

$$\underline{y}_P(t) = \sum_{n=-\infty}^{\infty} y_n \mathrm{e}^{in\Omega t} \tag{13}$$

$$\underline{f}(t) = \sum_{n=-\infty}^{\infty} f_n \mathrm{e}^{in\Omega t} \tag{14}$$

where Ω is the fundamental frequency and $i^2 = -1$. In the following developments, we assume that Ω is very close to Ω_0 formulated as:

$$\omega = 1 + \sigma\varepsilon \tag{15}$$

where $\omega = \dfrac{\Omega}{\Omega_0}$. We can rewrite Eq. 6:

$$\underline{\theta}'' + \varepsilon \underline{c_\theta} \underline{\theta}' + \frac{\sin(\sqrt{\varepsilon}\underline{\theta})}{\sqrt{\varepsilon}} + \varepsilon \cos(\sqrt{\varepsilon}\underline{\theta}) \underline{x}_P'' + \sqrt{\varepsilon} \sin(\sqrt{\varepsilon}\underline{\theta}) \underline{y}_P'' = \varepsilon \cos(\sqrt{\varepsilon}\underline{\theta}) \underline{f} \tag{16}$$

where $'$ designates the derivation with respect to dimensionless time τ. In the multiple scale method, we split the time in several scales thanks to the small parameter ε:

$$\tau_n = \varepsilon^n \tau, \ n \in \mathbb{N} \tag{17}$$

Thus, we redefine the derivative operator:

$$\frac{\mathrm{d}}{\mathrm{d}\tau} = \sum_{n \in \mathbb{N}} \varepsilon^n \frac{\partial}{\partial \tau_n} \tag{18}$$

Then, we introduce the complex variable of Manevitch [44]:

$$\Theta \mathrm{e}^{i\omega\tau} = \underline{\theta}' + i\omega\underline{\theta} \tag{19}$$

In our analysis, we are interesting only in the first harmonic of the response of the system. For an arbitrary function of the system $h(\tau_0, \tau_1, \tau_2, ...)$, this is performed by:

$$H = \frac{\omega}{2\pi} \int_0^{\frac{2\pi}{\omega}} h(\tau_0, \tau_1, \tau_2, ...) \mathrm{e}^{-i\omega\tau_0} \mathrm{d}\tau_0 \tag{20}$$

2.4.1 System behavior at different timescales

At fast timescale τ_0, i.e. at order ε^0 the analysis gives:

$$\frac{\partial \Theta}{\partial \tau_0} = 0 \tag{21}$$

which means that the system does not vary at fast timescale. At slow timescale τ_1, i.e. at order ε^1 the equation reads:

$$\frac{\partial \Theta}{\partial \tau_1} + \left(\frac{\underline{c_\theta}}{2} + i\sigma \right) \Theta + \frac{i}{16} \Theta \left| \Theta \right|^2 - h_1 - 2iy_2 \Theta^* = 0 \tag{22}$$

where $h_1 = x_1 + f_1$ and * stands for the complex conjugate of the argument. We can make several remarks. First we note that the horizontal component of the base and the external excitations, respectively, $\underline{x}_P$ and F have the same effect on the pendulum. Then, only the fundamental harmonic of the horizontal excitation affects the dynamic of the pendulum, whereas only the second harmonic of the parametric excitation (vertical) influences the pendulum behavior. Finally, thanks to the rescaling of θ with $\sqrt{\varepsilon}$ (Eq. 7) the first nonlinear term of the expansion of $\sin(\theta)$ in form of series enters to system equation at this timescale. So, in this case, a part of nonlinear behavior of the pendulum is taken into account.

2.4.2 Equilibrium points

We seek for the asymptotic state of the system when $\tau_1 \to \infty$, so $\dfrac{\partial \Theta}{\partial \tau_1} = 0$ corresponding to the equilibrium points of the system. The complex variables can be written in the polar form as: $\Theta = N_\theta \mathrm{e}^{i\delta_\theta}$, $h_1 = \left| h_1 \right| \mathrm{e}^{i\delta_h}$ and $y_2 = \left| y_2 \right| \mathrm{e}^{i\delta_y}$. The Eq. 22 becomes:

$$\left(\frac{\underline{c_\theta}}{2} + i\sigma \right) N_\theta + \frac{i}{16} N_\theta^3 - \left| h_1 \right| \mathrm{e}^{i(\delta_h - \delta_\theta)} - 2i \left| y_2 \right| N_\theta \mathrm{e}^{i(\delta_y - 2\delta_\theta)} = 0 \tag{23}$$

The real and imaginary parts of the equation 23 read:

$$\frac{\underline{c_\theta}}{2} N_\theta = \left| h_1 \right| \cos(\delta_h - \delta_\theta) + 2 \left| y_2 \right| N_\theta \sin(\delta_y - 2\delta_\theta) \tag{24}$$

$$\sigma N_\theta + \frac{1}{16} N_\theta^3 = \left| h_1 \right| \sin(\delta_h - \delta_\theta) + 2 \left| y_2 \right| N_\theta \cos(\delta_y - 2\delta_\theta) \tag{25}$$

Equations 24 and 25 lead to the following polynomial equation in N_θ:

$$\frac{1}{256}N_\theta^6 + \frac{\sigma}{8}N_\theta^4 + \left(\sigma^2 + \frac{\underline{c}_\theta^2}{4} - 4\left|y_2\right|^2\right)N_\theta^2 - 4\left|h_1\right|\left|y_2\right|\sin(\delta_\theta + \delta_h - \delta_y)N_\theta - \left|h_1\right|^2 = 0 \tag{26}$$

To determine the stability of each equilibrium point, we linearly perturb variables of Eq. 22 as:

$$N_\theta \to N_\theta + \Delta N_\theta \tag{27}$$

$$\delta_\theta \to \delta_\theta + \Delta\delta_\theta \tag{28}$$

After linearization, we obtain the following equation:

$$\begin{pmatrix} \dfrac{\partial \Delta N_\theta}{\partial \tau_1} \\ N_\theta \dfrac{\partial \Delta\delta_\theta}{\partial \tau_1} \end{pmatrix} = \mathbf{D}\begin{pmatrix} \Delta N_\theta \\ \Delta\delta_\theta \end{pmatrix} \tag{29}$$

- If $h_1 = 0$

$$\mathbf{D} = \begin{bmatrix} 2\left|y_2\right|\sin(2\delta_\theta - \delta_y) - \dfrac{c_\theta}{2} & 4N_\theta\left|y_2\right|\cos(2\delta_\theta - \delta_y) \\ -\dfrac{N_\theta^2}{8} & -4N_\theta\left|y_2\right|\sin(2\delta_\theta - \delta_y) \end{bmatrix} \tag{30}$$

- If $h_1 \neq 0$ then $N_\theta \neq 0$ and

$$\mathbf{D} = \begin{bmatrix} 2\left|y_2\right|\sin(2\delta_\theta - \delta_y) - \dfrac{c_\theta}{2} & 4N_\theta\left|y_2\right|\cos(2\delta_\theta - \delta_y) - \left|h_1\right|\sin(\delta_\theta - \delta_h) \\ -\dfrac{N_\theta^2}{8} - \dfrac{\left|h_1\right|}{N_\theta}\sin(\delta_\theta - \delta_h) & -4N_\theta\left|y_2\right|\sin(2\delta_\theta - \delta_y) - \left|h_1\right|\cos(\delta_\theta - \delta_h) \end{bmatrix} \tag{31}$$

If the real part of eigenvalues of the matrix $\mathbf{D}$ is both negative, the equilibrium point is stable, otherwise, it is unstable.

2.4.3 Phase portrait

By taking the real and imaginary parts of Eq. 22, we can write after linearization the following equation:

$$\mathbf{M}\begin{pmatrix} \dfrac{\partial N_\theta}{\partial \tau_1} \\ \dfrac{\partial \delta_\theta}{\partial \tau_1} \end{pmatrix} = \begin{pmatrix} f_1(N_\theta, \delta_\theta) \\ f_2(N_\theta, \delta_\theta) \end{pmatrix} \tag{32}$$

For any state of the system described by $(\delta_\theta, N_\theta)$, we can determine the direction of the flow in the $(\delta_\theta, N_\theta)$ plan by inverting the matrix $\mathbf{M}$.
For all the following examples, we take $\underline{c}_\theta = 0.25$ and $\varepsilon = 10^{-2}$.

2.5 Effects of the horizontal component of the base excitation

First we consider only a horizontal excitation of the pendulum ($y_2 = 0$). The amplitudes of equilibrium points N_θ are solutions of a polynomial of degree 6 given by Eq. 26. They are traced in Fig. 2 for several values of $|h_1|$. The value of the resonance frequency decreases when $|h_1|$ increases. This is a softening effect of the pendulum system [45] .

We can describe the skeleton curve traced on the Fig. 2 by the the following system of equations:

$$\begin{cases} \sigma = -\left(\dfrac{\left|h_1\right|}{2\underline{c}_\theta}\right)^2 \\ N_\theta = \dfrac{2\left|h_1\right|}{\underline{c}_\theta} \end{cases} \tag{33}$$

For particular excitation of amplitude h_1 and frequency σ, we can trace a phase portrait. Figure 3 shows an example with $h_1 = 0.5$ and $\sigma = -0.7$. In this state, the system presents two stables equilibrium points and one unstable equilibrium point.

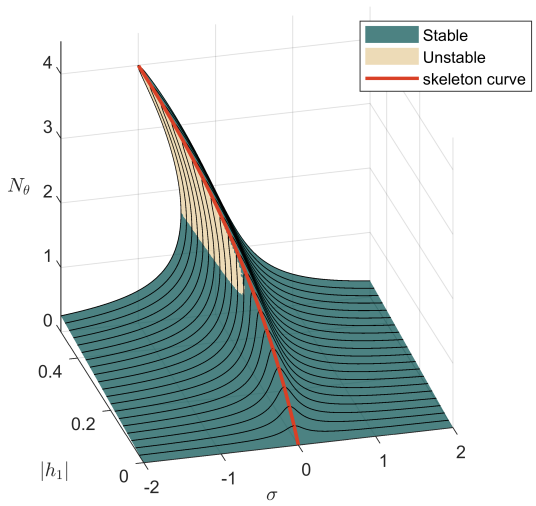

Figure 2: Equilibrium points of the reference system as a function of σ and horizontal excitation h_1. Stable and unstable zones are identified.

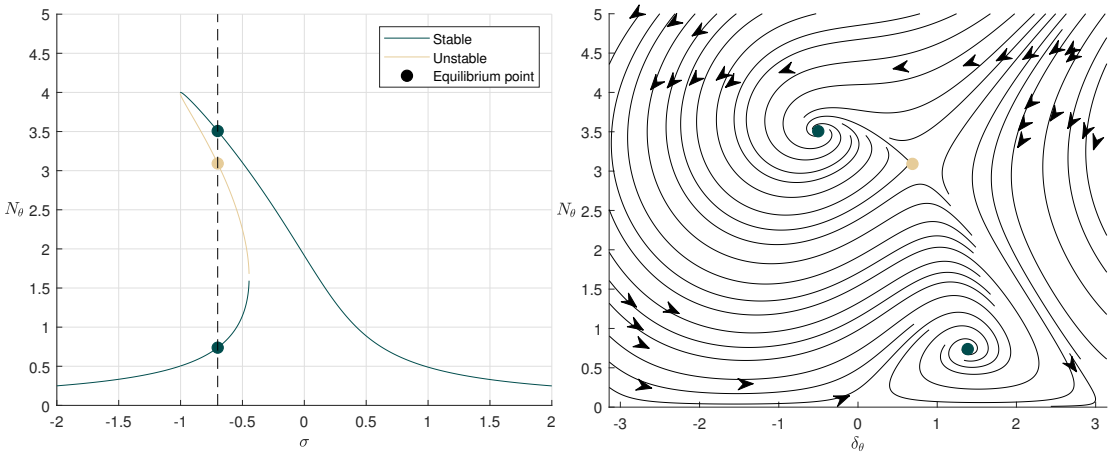

(a) (b)

Figure 3: Equilibrium points (3a) and phase portrait (3b) of the system for $h_1 = 0.5$ and $\sigma = -0.7$.

2.6 Effects of the parametric excitation (vertical component of the base excitation)

Here we consider only vertical excitation, i.e., $h_1 = 0$. The equation 26 becomes:

$$\left[\frac{1}{256}N_\theta^4 + \frac{\sigma}{8}N_\theta^2 + \left(\sigma^2 + \frac{c_\theta^2}{4} - 4\left|y_2\right|^2\right)\right]N_\theta^2 = 0 \tag{34}$$

We deduct that $N_\theta = 0$ is always an equilibrium point. Other solutions exist if $c_\theta < 4\left|y_2\right|$:

$$N_\theta = 2\sqrt{2\left(\pm\sqrt{16\left|y_2\right|^2 - c_\theta^2} - 2\sigma\right)} \tag{35}$$

In the plan (σ, N_θ), Eq. 35 describes two branches represented in Fig. 4. It is seen that stable branches of the system can correspond to high amplitude levels of N_θ. The unstable branch and the stable branch cut the axis $N_\theta = 0$ at the respective coordinate:

$$\sigma_{\mathrm{u}} = -\frac{1}{2}\sqrt{16\left|y_2\right|^2 - c_\theta^2} \qquad \sigma_{\mathrm{s}} = \frac{1}{2}\sqrt{16\left|y_2\right|^2 - c_\theta^2} \tag{36}$$

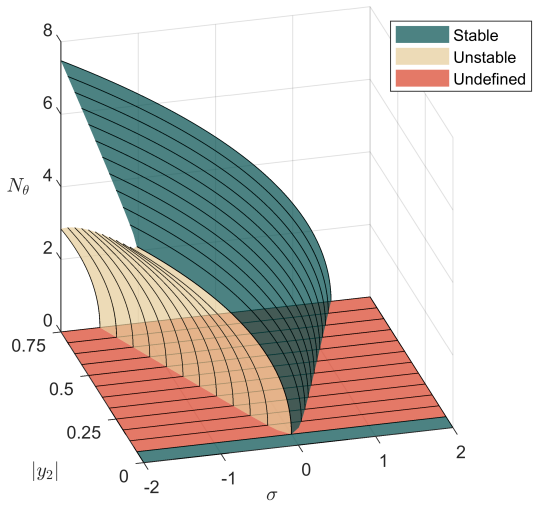

Figure 4: Equilibrium points of the reference system as a function of σ and vertical excitation y_2. Stable and unstable zones are identified. The stability is not determined when it depends on the phase difference.

When the amplitude of an equilibrium point is zero ($N_\theta = 0$), its phase δ_θ is unknown. However, in the perturbation method (Eq. 28), $\delta_\theta = \Delta\delta_\theta$. In this case, the eigenvalues μ_k of the matrix $\mathbf{D}$ are:

$$\mu_1 = 0 \tag{37}$$

$$\mu_2 = 2\,|y_2|\sin(2\delta_\theta - \delta_y) - \frac{\varsigma_\theta}{2} \tag{38}$$

When $|y_2| > \varsigma_\theta/4$, the stability depends on $2\delta_\theta - \delta_y$. The Fig. 4 shows the equilibrium point as a function of amplitude N_θ and $|y_2|$. On this representation, the stability remains undefined. The response curve of the system for an excitation $y_2 = 0.4$ and $\sigma = -1$ (Fig. 5a) shows three

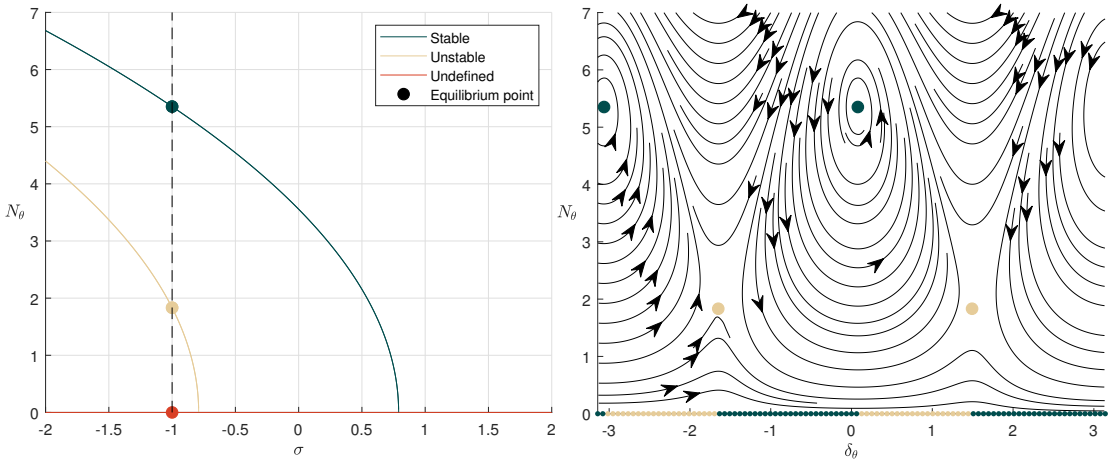

(a) (b)

Figure 5: Equilibrium points (5a) and phase portrait (5b) of the system for $y_2 = 0.4$ and $\sigma = -1$.

equilibrium points: one is stable, one is unstable, whereas the stability of the last one remains unknown. On the phase portrait (Fig. 5b), the nonzero equilibrium points appear twice because of the periodicity of π in δ_θ visible in Eq. 23. The phase portrait shows also the dependence of the stability of the equilibrium point with zero amplitude to the phase of the perturbation introduced in the equation of the system.

2.7 The general case

The system of Eqs. 25 and 24 can be solved numerically to find the equilibrium points of the system when $h_1 \neq 0$ and $y_2 \neq 0$. Figure 6 shows the results for given values of h_1 and y_2. There is no more solution with zero amplitude. Each branch of the curve with vertical excitation is split in two branches. The equilibrium points of the new branches have a difference of phase close to π as seen on the phase portrait (Fig. 6b).

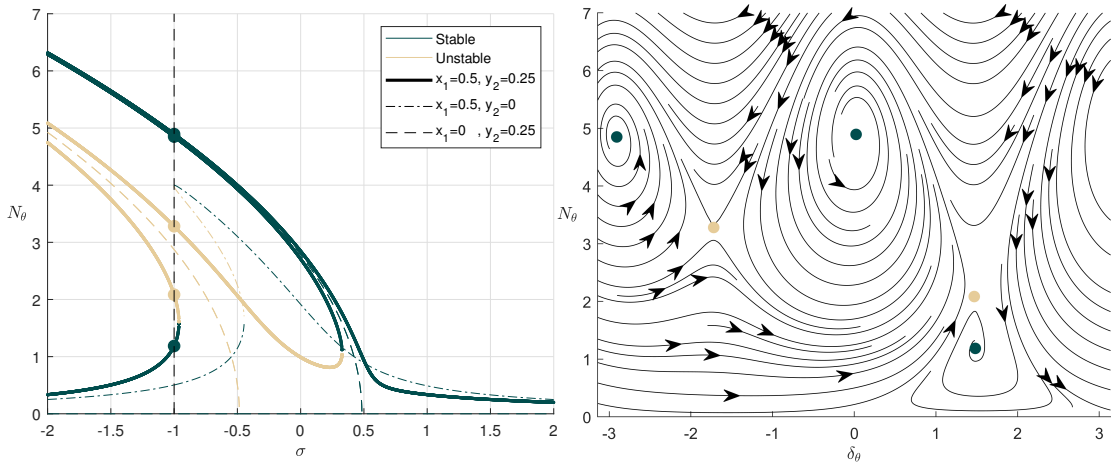

(a) (b)

Figure 6: Equilibrium points (6a) and phase portrait (6b) of the reference system for $h_1 = 0.5$, $y_2 = 0.25$ and $\sigma = -1$.

3 Pendulum and a coupled nonlinear absorber

3.1 The mechanical system

Here, a nonlinear absorber is attached to the pendulum on the point A located at a distance l from P as seen in Fig. 7. The mass m of the absorber is very small compared to the mass of the pendulum M. In the multiple scale method, we take the small parameter ε equal to the ratio of mass:

$$\varepsilon = \frac{m}{M} \ll 1 \tag{39}$$

A nonlinear restoring force function s which is purely nonlinear links this mass to the pendulum:

$$s(u) = Ku^3 \tag{40}$$

where u is the relative distance between the absorber and the pendulum. The damping coefficient of the absorber is C_u.

3.2 Governing system equations

The coordinates of the mass of the absorber m read:

$$\begin{cases} x_m = X_P + l\sin(\theta) + u\cos(\theta) \\ y_m = Y_P - l\cos(\theta) + u\sin(\theta) \end{cases} \tag{41}$$

The kinetic $\mathcal{K}$ and potential $\mathcal{U}$ energies of the system became:

$$\mathcal{K} = \frac{1}{2}J\dot{\theta}^2 + \frac{1}{2}M\left(\dot{x}_G^2 + \dot{y}_G^2\right) + \frac{1}{2}m\left(\dot{x}_m^2 + \dot{y}_m^2\right) \tag{42}$$

$$\mathcal{U} = Mgy_G + mgy_m + \frac{1}{4}Ku^4 \tag{43}$$

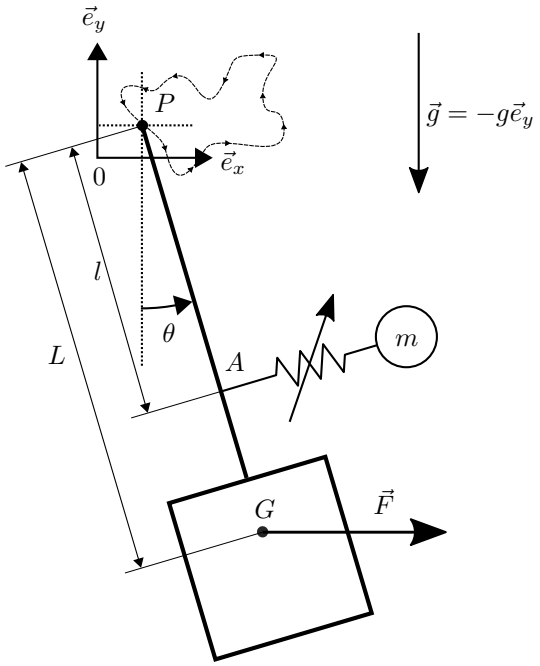

Figure 7: Pendulum coupled with an nonlinear absorber in a gravity field $\vec{g}$ excited by a force $\vec{F}$ and the displacement of its center P.

The nonconservative internal forces of the system are:

$$F_\theta = -C_\theta \dot{\theta} + FL\cos(\theta) \tag{44}$$

$$F_u = -C_u \dot{u} \tag{45}$$

We deduct from Eqs. 41-45 with the Lagrange equations, the dynamic equations of the system:

$$\begin{cases} \left[1 + \dfrac{\varepsilon}{\gamma}(\lambda^2 + \nu^2)\right]\theta'' + \underline{c_\theta}\theta' + (1+\varepsilon\lambda)\sin(\theta) + \varepsilon\dfrac{\lambda}{\gamma}\nu'' + 2\dfrac{\varepsilon}{\gamma}\theta'\nu'\nu + \varepsilon\cos(\theta)\nu \\ \quad + \left[\cos(\theta) + \varepsilon\left(\lambda\cos(\theta) - \nu\sin(\theta)\right)\right]x_P'' + \left[\sin(\theta) + \varepsilon\left(\lambda\sin(\theta) + \nu\cos(\theta)\right)\right]y_P'' \\ \qquad = f\cos(\theta) \\ \varepsilon\left[\lambda\theta'' + \nu'' - \theta'^2\nu + c_u\nu' + \gamma\left(\sin(\theta) + \cos(\theta)x_P'' + \sin(\theta)y_P''\right)\right] + k\nu^3 = 0 \end{cases} \tag{46}$$

where $\gamma = \dfrac{j}{L} + 1 = \dfrac{J}{ML^2} + 1$, $\lambda = \dfrac{l}{L}$, $\nu = \dfrac{u}{L}$, $c_u = \dfrac{C_u}{m\Omega_0}$ and $k = \dfrac{K}{ML^2\Omega_0^2}$.

3.3 System behavior at fast timescale: ε^0 order of system equations.

To analyze the equation of the system with the multiple scale method we assume that the displacement of the absorber is small:

$$\nu = \sqrt{\varepsilon}\underline{\nu} \tag{47}$$

We introduce another variable of Manevitch [44]:

$$U\mathrm{e}^{i\omega t} = \nu' + i\omega\nu \tag{48}$$

By keeping only the first harmonics, we find at fast time τ_0:

$$\frac{\partial\Theta}{\partial\tau_0} = 0 \tag{49}$$

$$\frac{\partial U}{\partial\tau_0} = -\frac{c+i}{2}U - \frac{i\left(\lambda-\gamma\right)}{2}\Theta + i\frac{3k}{8}\left|U\right|^2 U = \mathcal{H} \tag{50}$$

We seek for the asymptotic state of the system when $\tau_0 \to \infty$ or $\dfrac{\partial U}{\partial \tau_0} = \mathcal{H} = 0$. Equation 50 gives the equation of the slow invariant manifold (SIM):

$$(\lambda - \gamma)^2 N_\theta^2 = \left(\frac{3k}{4} N_u^3 - N_u\right)^2 + c_u^2 N_u^2 \tag{51}$$

Figure 8 shows the curve of the SIM for $k = 1$, $c_u = 0.25$, $\lambda = 0.8$ and $\gamma = 0.25$. In all the following examples, the parameters of the nonlinear absorber do not change. We check the

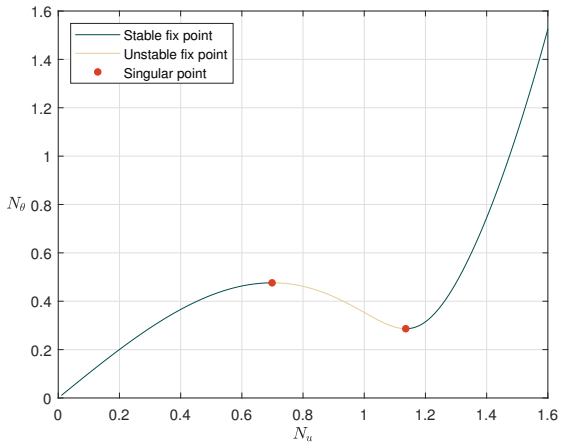

Figure 8: The SIM of coupled system.

stability of the SIM with a perturbation method. We introduce in Eq. 50 a small perturbation of U:

$$U \to U + \Delta U, \ \Delta U \ll U \tag{52}$$

After linearization, we get the following equation:

$$\begin{pmatrix} \dfrac{\partial \Delta U}{\partial \tau_0} \\ \dfrac{\partial \Delta U^*}{\partial \tau_0} \end{pmatrix} = \frac{1}{2} \begin{bmatrix} M_1 & M_2 \\ M_2^* & M_1^* \end{bmatrix} \begin{pmatrix} \Delta U \\ \Delta U^* \end{pmatrix} \tag{53}$$

with

$$M_1 = \frac{3ik}{2} |U|^2 - i - c_u \tag{54}$$

$$M_2 = \frac{3ikU^2}{4} \tag{55}$$

In order to know the stability of the SIM, we check the sign of the eigenvalues μ of the matrix $\mathbf{M}$. Its characteristic equation reads:

$$\mu^2 - (M_1 + M_1^*)\mu + |M_1|^2 - |M_2|^2 = 0 \tag{56}$$

The sum and the product of the roots of this polynomial $\mu_{1,2}$ are equal to $M_1 + M_1^*$ and $|M_1|^2 - |M_2|^2$ respectively:

$$\mu_1 + \mu_2 = -2c_u < 0 \tag{57}$$

$$\mu_1 \mu_2 = \frac{27k^2}{16} N_u^4 - 3kN_u^2 + c_u^2 + 1 \tag{58}$$

We conclude the SIM is unstable if $\mu_1 \mu_2 < 0$. If $c_u \geq \dfrac{1}{3}$, the SIM is entirely stable. Otherwise, the SIM is unstable if:

$$\frac{8 - 4\sqrt{1 - 3c_u^2}}{9k} < N_u^2 < \frac{8 + 4\sqrt{1 - 3c_u^2}}{9k} \tag{59}$$

The stable and unstable zones of the SIM are identified in Fig. 8.

3.4 System behavior at slow timescale: ε^1 order of system equations.

At the next order ε^1, the first equation of the system 46 gives:

$$\frac{\partial \Theta}{\partial \tau_1} + \left(i\sigma + \frac{c_\theta - i\lambda}{2} + \frac{i\lambda^2}{2\gamma} \right) \Theta + \frac{i}{16} |\Theta|^2 \Theta + \frac{i}{2} \left(\frac{\lambda}{\gamma} - 1 \right) U - h_1 - 2iy_2\Theta^* \tag{60}$$

The equilibrium points are also fix points, so they are the solution of the system composed of Eqs. 60 and 50.

3.4.1 Stability of equilibrium points

Equation 50 gives the expression of Θ as a function of U:

$$\Theta = \frac{1}{\lambda - \gamma} \left(i\frac{3k}{4} |U|^2 + ic - 1 \right) U \tag{61}$$

We replace Eq. 61 in Eq. 60 to obtain an expression of the variation of Θ as a function of δ_u and N_u:

$$\frac{\partial \Theta}{\partial \tau_1} = \frac{e^{i\delta_u}}{\lambda - \gamma} \left[\left(i\frac{3k}{4} N_u^2 - i - c \right) N_u \frac{\partial \delta_u}{\partial \tau_1} + \left(\frac{9k}{4} N_u^2 + ic - 1 \right) \frac{\partial N_u}{\partial \tau_1} \right] = \mathcal{F}(\delta_u, N_u) \tag{62}$$

By taking real and imaginary parts of Eq. 62, we can write the following matrix equation:

$$\mathbf{A} \begin{pmatrix} \dfrac{\partial \delta_u}{\partial \tau_1} \\ \dfrac{\partial N_u}{\partial \tau_1} \end{pmatrix} = \begin{pmatrix} \mathcal{F}_1(\delta_u, N_u) \\ \mathcal{F}_2(\delta_u, N_u) \end{pmatrix} \tag{63}$$

By introducing small perturbations $\Delta\delta_u$ and ΔN_u in corresponding variables and after linearization we can write:

$$\mathbf{A} \begin{pmatrix} \dfrac{\partial \Delta\delta_u}{\partial \tau_1} \\ \dfrac{\partial \Delta N_u}{\partial \tau_1} \end{pmatrix} = \mathbf{B} \begin{pmatrix} \Delta\delta_u \\ \Delta N_u \end{pmatrix} \tag{64}$$

We can deduce the stability with the signs of the eigenvalues of the matrix $\mathbf{A}^{-1}\mathbf{B}$. Equilibrium points can coincide with singular points of the system (so forming fold singularities), if they verify the following equation [46]:

$$\det(\nabla_{(U,U^*)}\mathcal{H}) = - \begin{vmatrix} M_1 & M_2 \\ M_2^* & M_1^* \end{vmatrix} = 0 \tag{65}$$

where $\nabla_{(U,U^*)}\mathcal{H}$ stands for the Jacobian matrix of $\mathcal{H}$ versus variables U and U^*. We conclude that the fold singular equilibrium points are located at the borders between stable and unstable zones visible in Fig. 8.

3.4.2 Phase portraits

We use Eq. 63 to calculate the direction of the flow of the system in every point and trace the phase portrait in (δ_u, N_u). The Eq. 51 gives the expression of N_u^2 as a solution of a polynomial of degree 3. The three positive solutions correspond to the three zones of the SIM separated by fold singularities (see Fig. 8). In order to verify the efficiency of the nonlinear absorber, we plot phase portraits of the system. To represent the path of the system, we need to consider only the two solutions corresponding to the stable zones $N_{u1}(N_\theta^2)$ and $N_{u2}(N_\theta^2)$. We can express the value of δ_u as a function of N_u and Θ from Eq. 50:

$$\mathrm{e}^{i\delta_u} = \frac{\lambda - \gamma}{N_{u(1,2)} \left(\dfrac{3k}{4} N_{u(1,2)}^2 + ic - 1 \right)} \Theta \tag{66}$$

These solutions $U_{1,2} = \left(N_u e^{i\delta_u}\right)_{1,2}$ are replaced in Eq. 60:

$$\frac{\partial \Theta}{\partial \tau_1} = \left(\frac{\partial N_\theta}{\partial \tau_1} + iN_\theta \frac{\partial \delta_\theta}{\partial \tau_1}\right) e^{i\delta_\theta} = \mathcal{G}(\delta_\theta, N_\theta) \tag{67}$$

By taking the real and the imaginary parts of Eq. 67 we can calculate the direction of the system for each point $(\delta_\theta, N_\theta)$ and trace the phase portrait.

3.5 Effects of the horizontal component of the base excitation

Let us consider horizontal components of external and base excitations. From Eq. 62, we find N_u^2 as a solution of a polynomial of degree 9. Figure 9 shows the amplitudes N_u and N_θ of the equilibrium points of the system as a function of σ and $|h_1|$. Two unstable zones are visible. One was already present in the reference system (Fig. 2), whereas the other one corresponds to the unstable zone of the SIM ($0.70 < N_u < 1.14$). By comparing Fig. 9b with Fig. 2, we can appreciate the efficiency of the nonlinear absorber: for $|h_1| < 0.3$ the value of N_θ stays below 0.5. Figure 10 shows an example of a phase portrait for a given value of σ. On the phase

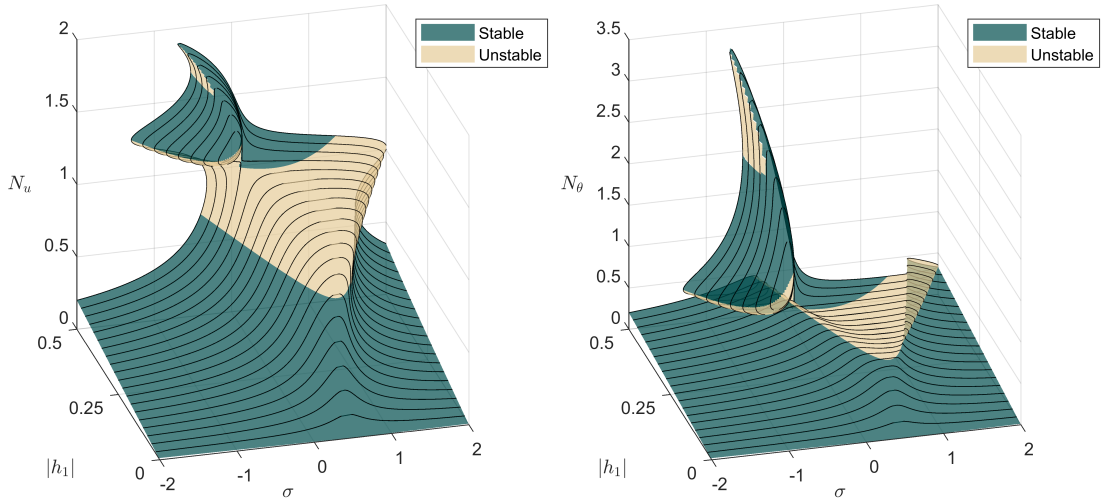

(a) N_u (b) N_θ

Figure 9: Amplitude N_u and N_θ of the equilibrium points of the pendulum coupled with the nonlinear absorber as a function of σ and $|h_1|$.

portrait in (δ_u, N_u) (Fig. 10b), the three zones of the SIM are separated by horizontal bold lines corresponding to singular points. The zone between the singular points is unstable. The singular points are also visible on the phase portrait in $(\delta_\theta, N_\theta)$ (Fig. 10d). Here, for the sake of clarity, only stable zones are represented. They are superposed between singular points.

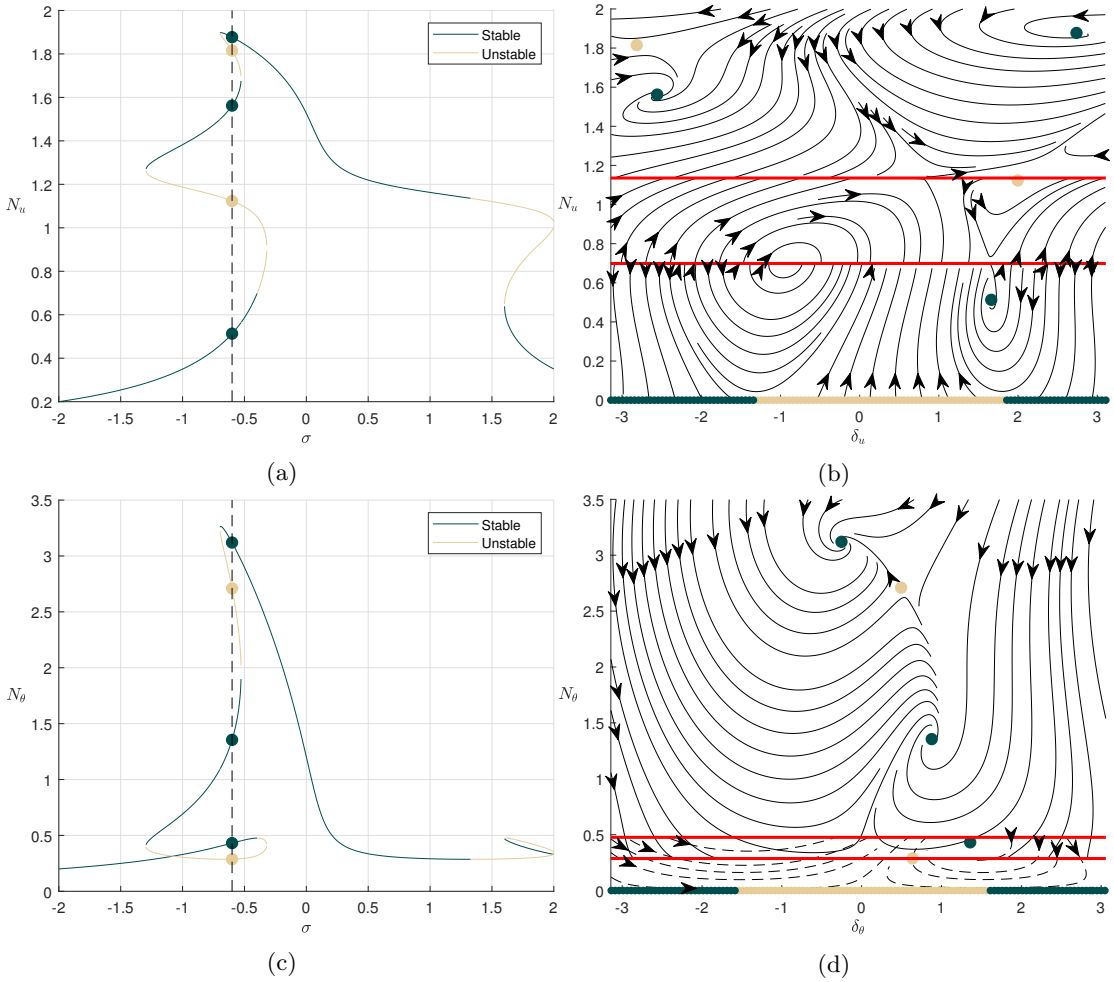

Figure 10: Amplitude N_u and N_θ of the equilibrium points of the pendulum coupled with the nonlinear absorber as a function of σ for $h_1 = 0.5$ and corresponding phase portraits for $\sigma = -0.6$.

3.6 Effects of the vertical component of the base excitation

Now, the same system is subjected to a vertical parametric excitation. From Eq. 62, the squared amplitudes N_u^2 of the equilibrium points are still a solution of a polynomial of degree 9. As in the reference model, the state $N_u = N_\theta = 0$ is an equilibrium point for any σ and y_2. For some values of $|y_2|$, the stability of these equilibrium points is undefined if we do not know the phase δ_u as shown in Fig. 11. The curves are split in two curves showing new equilibrium points. The amplitudes of equilibrium points with high value of N_θ are similar to the amplitudes of the equilibrium points of the reference system. The coordinates σ_s and σ_u of the intersection of the stable and unstable branches with the plan $N_u = 0$ are solution of a polynomial of degree 2, so we can know their analytic expressions as a function of $|y_2|$ (Fig. 12).

3.7 The general case

Equations 50 and 60 are solved numerically to trace the amplitudes N_u and N_θ of the equilibrium points in Fig. 13. As for the case without absorber, there is no solution with zero amplitude. The stable and unstable branches are split into two branches each. The equilibrium points of the new branches have similar amplitude but a difference of phase close to π.

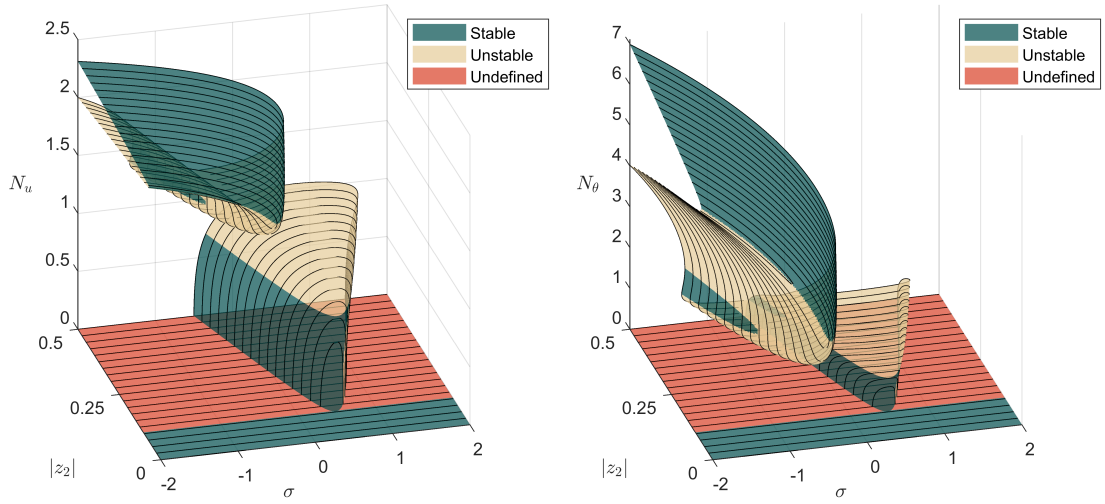

(a) N_u (b) N_θ

Figure 11: Amplitude N_u and N_θ of the equilibrium points of the pendulum coupled with the nonlinear absorber as a function of σ and y_2.

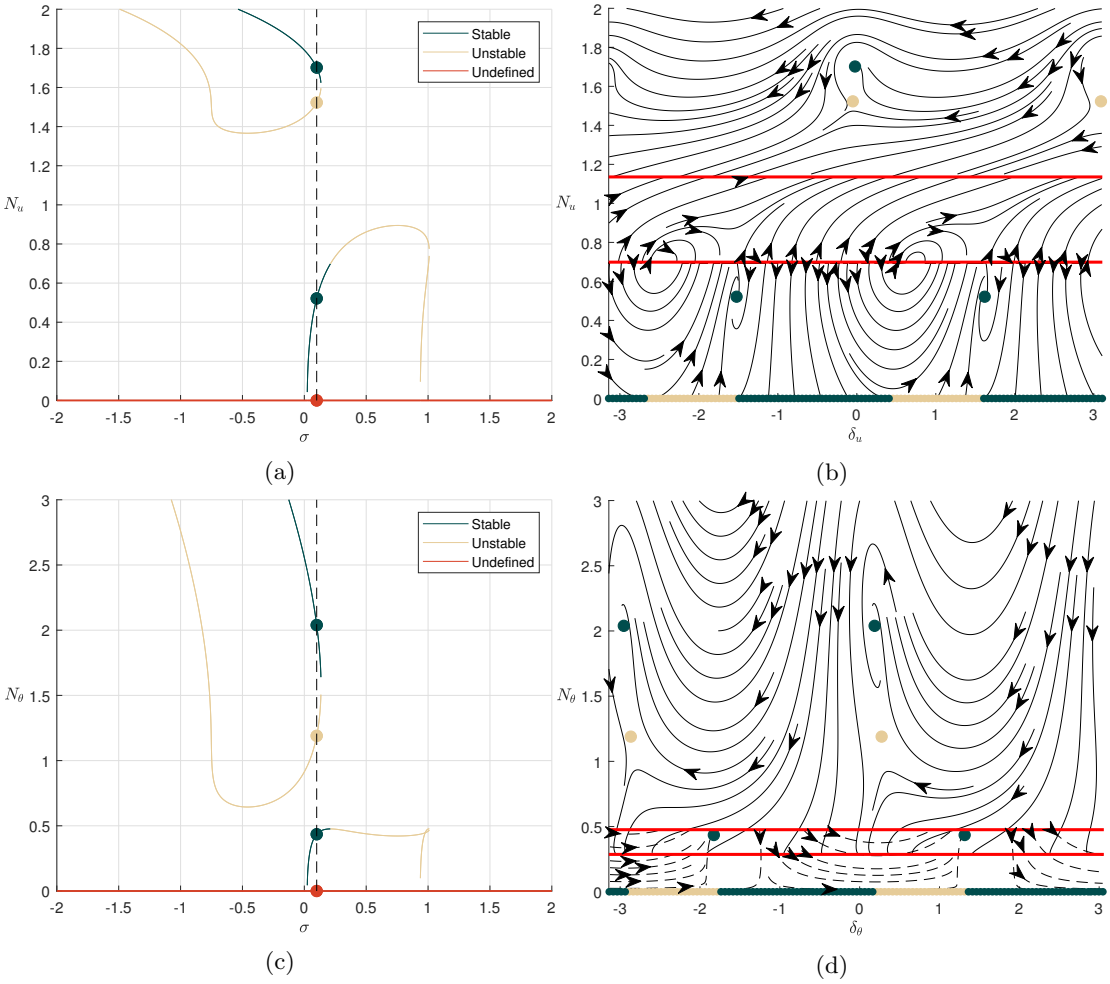

(a) (b)

(c) (d)

Figure 12: Amplitude N_u and N_θ of the equilibrium points of the pendulum coupled with the nonlinear absorber as a function of σ for $y_2 = 0.25$ and corresponding phase portraits for $\sigma = 0.1$.

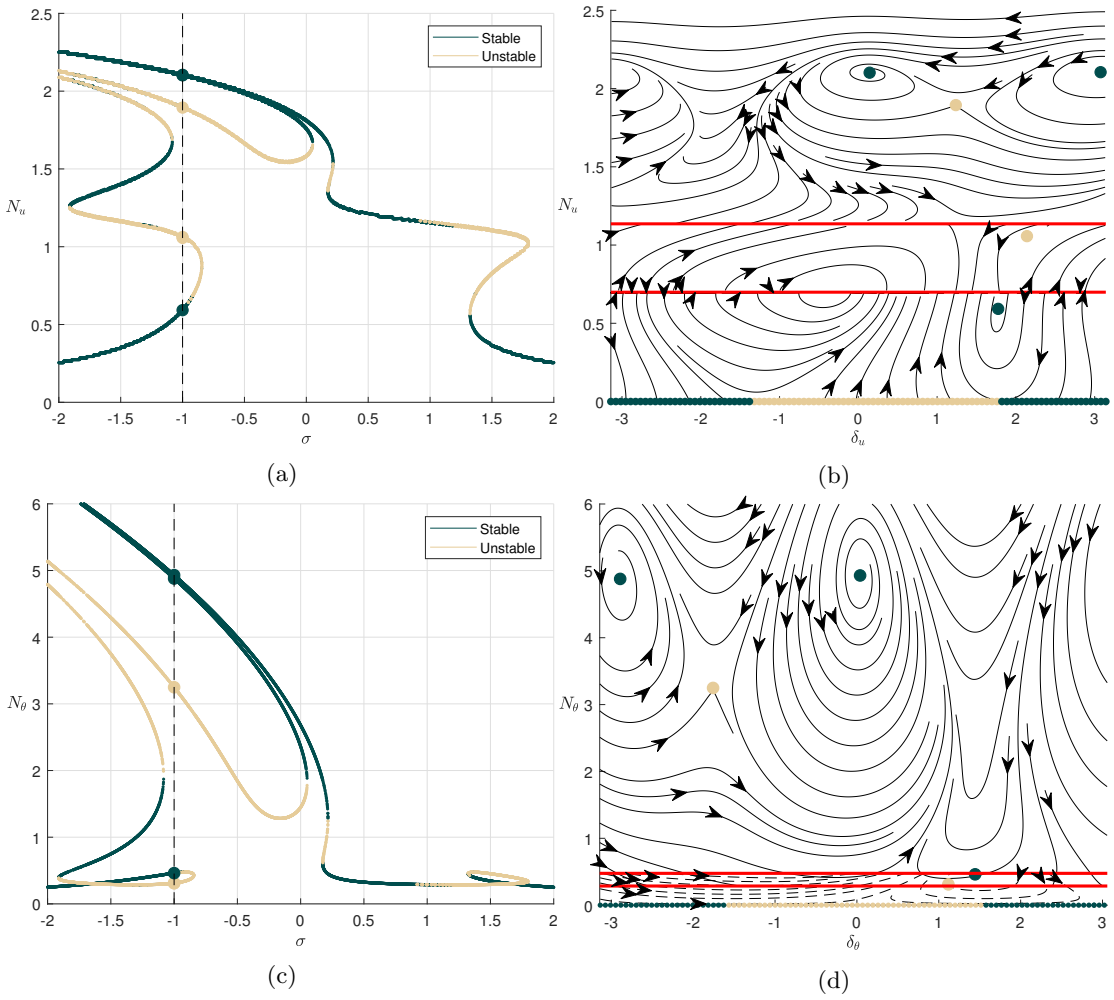

Figure 13: Amplitude N_u and N_θ of the equilibrium points of the pendulum coupled with the nonlinear absorber as a function of σ for $h_1 = 0.5$, $y_2 = 0.25$ and corresponding phase portraits for $\sigma = -1$.

4 The effect of the nonlinear absorber on the system

In this section all numerical results are obtained by integrating of Eq. 46 with ode45 algorithm of MATLAB with absolute error tolerance at 10^{-15} and relative error tolerance at 3×10^{-14}.

4.1 Horizontal excitations

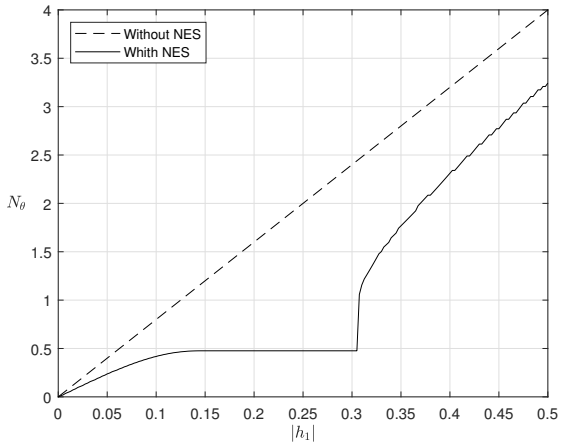

Figure 14: Comparison with and without nonlinear absorber of maximum amplitude of equilibrium point for all σ as a function of $|h_1|$.

In case of pure horizontal excitation, Fig. 14 compares the maximum value of the amplitude of the equilibrium point for any σ. The curve with nonlinear absorber is always under the curve of the reference system, but the efficiency is maximal for $|h_1| = 0.3$. We can see is a plateau $N_{\theta s} = 0.5$ corresponding to the value of the first singular point of the SIM (Fig. 8). The amplitude N_θ is thresholded by a phenomenon called strongly modulated response (SMR) [47]. As illustrated in Fig. 15, the system jumps from singular point to oscillate between both stable zones of the SIM .

When designing the nonlinear absorber, we consider the vibration of the pendulum is acceptable if $N_\theta < N_{\theta s}$. We consider also that the horizontal excitation $|h_1|$ can reach values that remain below 0.3. In the case of Fig. 16, the SMR oscillations appear and remain for a duration before the system goes to an equilibrium point. We define the Poincaré map:

$$P(n) = \Big(\theta(nT), \dot{\theta}(nT)\Big) \tag{68}$$

with $T = \dfrac{2\pi}{\omega}$. The Fig. 16b shows a Poincaré map corresponding to a numerical integration of the equations of the system. In this case, the system stays in a non-periodic state for a while ($\tau < 4000$) and then it goes to the stable equilibrium point. All initial points of coordinates $(\theta, \dot{\theta})$ from which the system goes to this equilibrium point are in the basin of attraction of this point. This basin is represented on the Fig. 17a.

For all initial points of the maps of Fig. 17a, a Poincaré section is traced in Fig. 17b. The points with high number of period are located in two different zones. First, the vicinity of the stable equilibrium point ($\theta = -0.036, \dot{\theta} = 0$) represents a periodic state of the system. It corresponds to the equilibrium point visible in Fig. 17a. The second zone is the ring around the previous point representing a quasi-periodic state. An example is given in Fig. 15 where SMR oscillations happen.

For the points that are not in the basin, the system stays in a SMR state for an infinite duration. For all the points of the basin, the system goes to the equilibrium point but not with

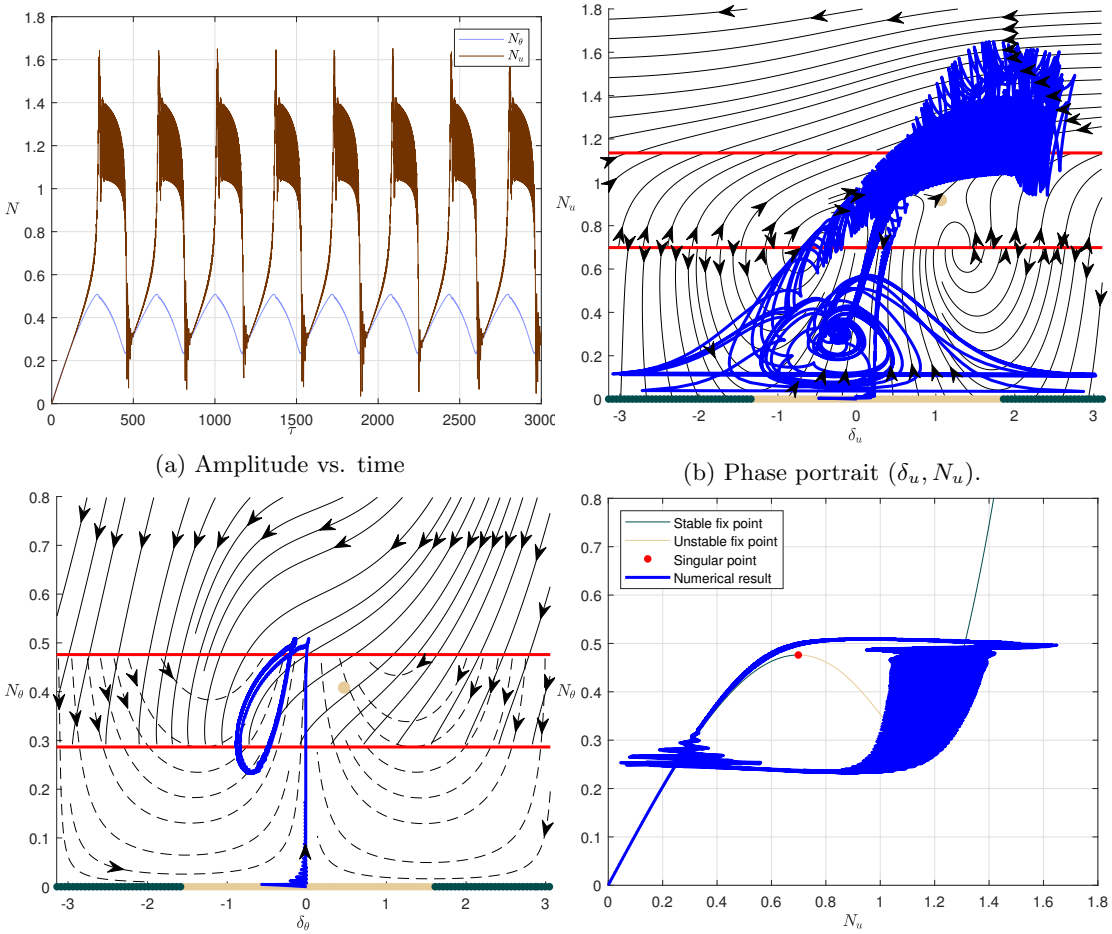

(a) Amplitude vs. time

(b) Phase portrait (δ_u, N_u).

(c) Phase portrait $(\delta_\theta, N_\theta)$.

(d) SIM

Figure 15: Numerical integration illustrating SMR phenomenon. Excitation: $h_1 = 0.25$, initial conditions: $\sigma = 0.5$, $\Theta(0) = 0$, $U(0) = 0$.

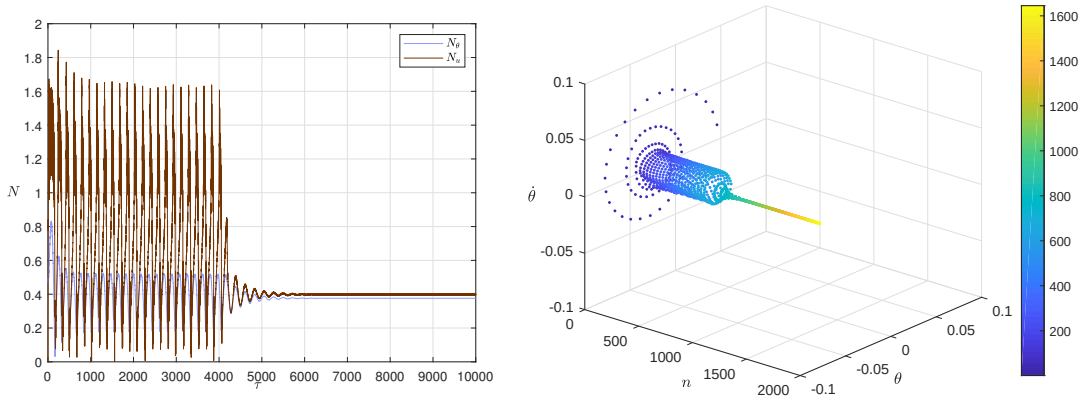

(a) Amplitudes as a function of time.

(b) Poincaré map of the evolution of the system.

Figure 16: Example of numerical integration with two phases: first SMR oscillations, then convergence to an equilibrium point. Color scale represents the number of periods n.

the same kinetic. To analyze this dynamic, we introduce a convergence criterion at r:

$$r(n) = |P(n) - P(n-1)| \tag{69}$$

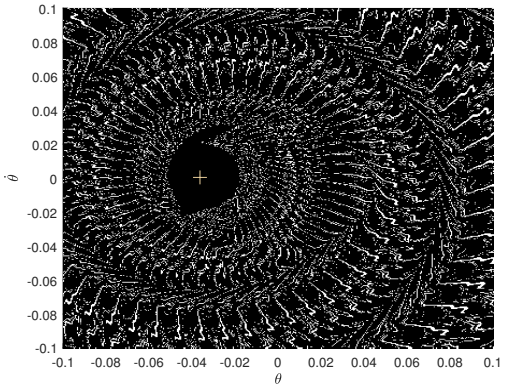

(a) Basin of attraction (dark zone) of the stable equilibrium point (cross).

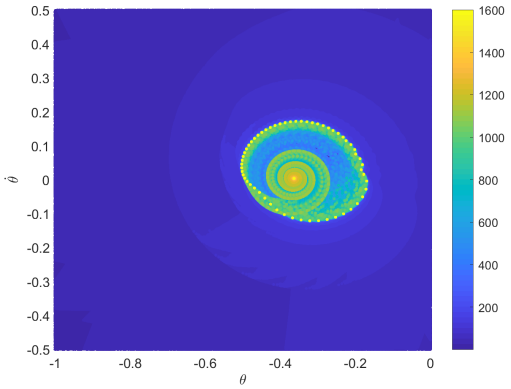

(b) Poincaré section of all initial points. Color scale represents the number of periods n.

Figure 17: Asymptotic behavior of the system versus its initial point for $h_1 = 1$ and $\sigma = 3.371$.

This criterion is represented in Fig. 18 for several values of n. In figures b and c, we can identify a zone around the equilibrium point for which the system converges rapidly to it. From the other points, the system is in a quasi-periodic state corresponding to the SMR oscillations. In Fig. 18d, after a very long time, the system converged for all points of its basin of attraction.

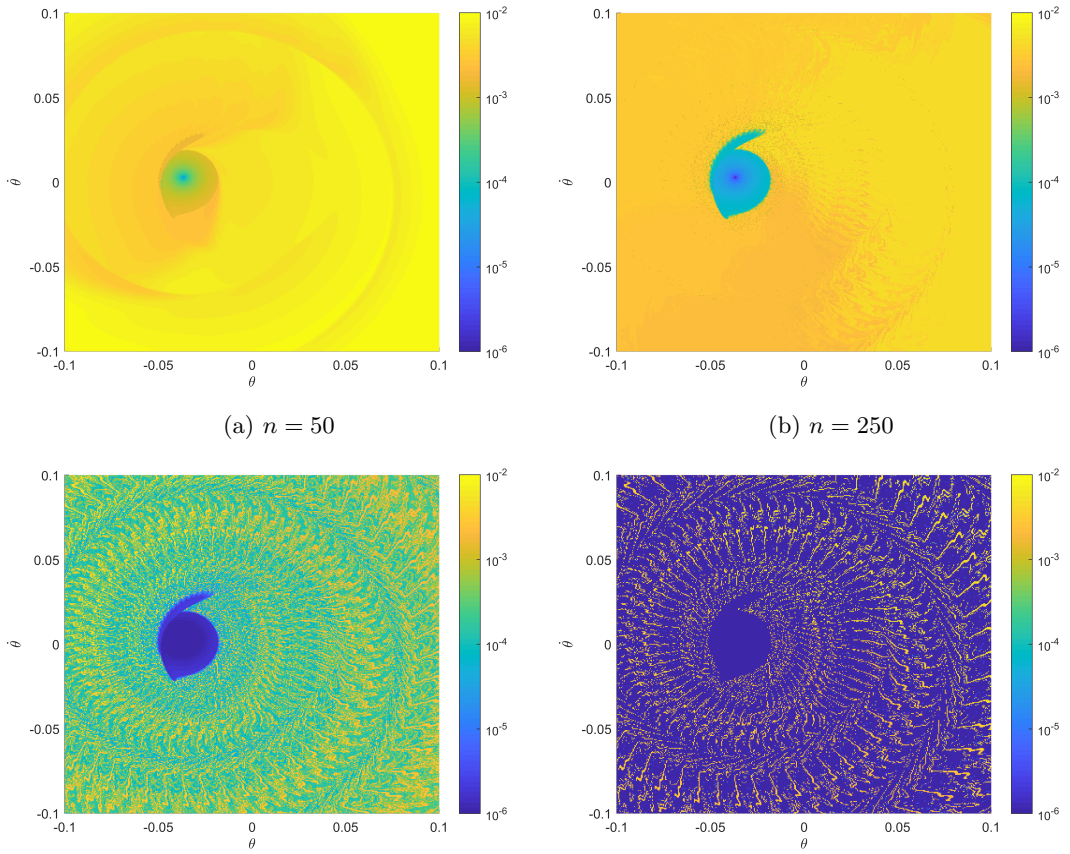

(a) $n = 50$

(b) $n = 250$

(c) $n = 500$

(d) $n = 1000$

Figure 18: Maps of convergence criterion r for different numbers of period (n). Colors represent the convergence criterion r.

4.2 Vertical excitation

Here the comparison of the maximum amplitude of the equilibrium point for a given excitation y_2 is not relevant because the amplitude N_θ tends to infinity when σ decreases. Of course, the model is no more valid for very low value of σ since we assumed the frequency of excitation is closed to the natural frequency of the pendulum. Moreover, for a given σ, the value of maximum amplitude of this stable equilibrium point is very similar as seen in Fig. 19.

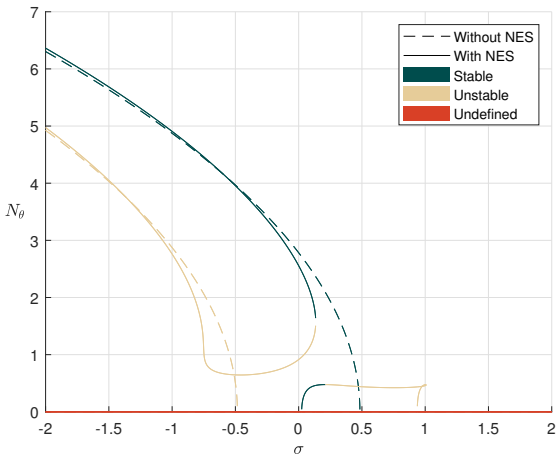

Figure 19: Comparison with and without nonlinear absorber of the amplitude of equilibrium point for $y_2 = 0.25$ as a function of σ.

On this figure, we can distinguish several domains:

- $\sigma < -0.8$: even though, coupling the system causes the main system experience higher amplitude compared with the system without absorber, the response of the system can be considered similar in both cases. In both cases, the presence of a stable equilibrium point with high amplitude is dangerous. The phase portrait of Fig. 20, shows that the system can reach the stable equilibrium point with high amplitude only for initial condition with $N_\theta > 1.5$. To confirm this conclusion, the basin of attraction of each stable equilibrium point is calculated numerically. For each numerical integration, we color the initial condition as a function of the final state of the system.

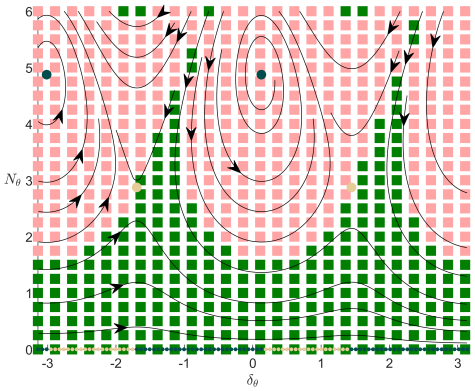

Figure 20: Basin of attraction of the equilibrium points of the system without nonlinear absorber for $y_2 = 0.25$ and $\sigma = -1$. For initial conditions corresponding to light squares ■, the system goes to the equilibrium point with high amplitude, for initial conditions corresponding to dark squares ■, the system goes to equilibrium point with zero amplitude.

- $-0.8 < \sigma < 0.1$, the maximum amplitude of stable equilibrium points are similar, but other equilibrium points with low amplitudes exist for coupled oscillators. The difference of behavior is visible on the phase portrait with basins of attraction traced in Fig. 21 for $\sigma = 0$. In the reference case, the system can reach a high amplitude equilibrium point, with an initial condition with an amplitude near to 0. With nonlinear absorber, the system cannot reach the high amplitude stable equilibrium point from an initial condition with an acceptable amplitude ($N_\theta(0) < 0.5$).
  The presence of an unstable equilibrium point with low amplitude creates a kind of barrier to the system. It is interesting to see in Fig. 11b that this zone is wider and wider, but the amplitude of this barrier do not vary when the excitation $|y_2|$ increases. This barrier is efficient for any value of the vertical excitation, whereas the nonlinear absorber is efficient until a maximum value of the horizontal excitation.

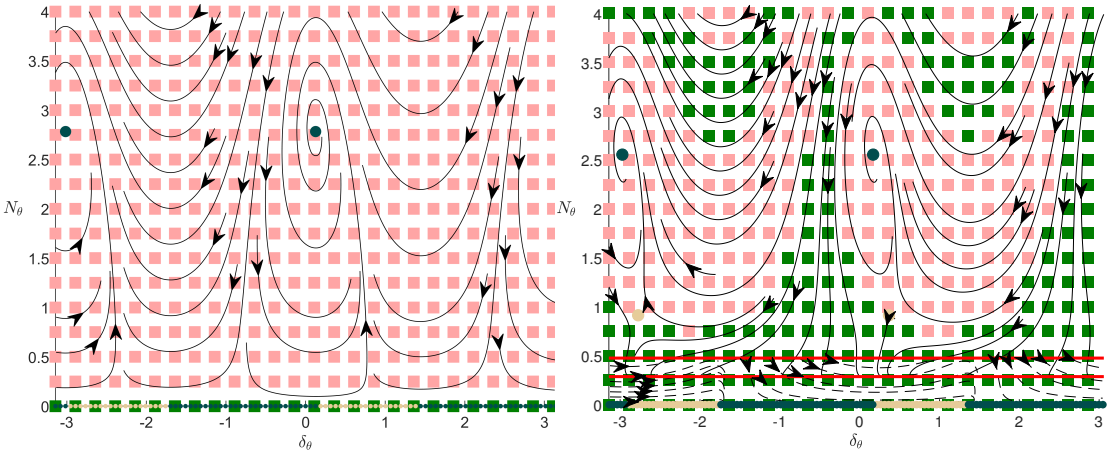

(a) Without nonlinear absorber

(b) With nonlinear absorber

Figure 21: Comparison of basin of attraction of the equilibrium points of the system without and with nonlinear absorber for $\sigma = 0$ and $y_2 = 0.25$. For initial conditions corresponding to light squares ■, the system goes to the equilibrium point with high amplitude, for initial conditions corresponding to dark squares ■, the system goes to equilibrium point with zero amplitude.

- $0.1 < \sigma < 1$, the equilibrium points with the nonlinear absorber have an acceptable amplitude ($N_\theta < 0.5$). This amplitude is below the threshold defined by the first singular point of the SIM ($N_{\theta s} = 0.5$). The SMR phenomenon can occur as seen in Fig. 22.
- $\sigma > 1$: all equilibrium points are zero.

To conclude, for low and high values of σ, the nonlinear absorber is not so efficient. When σ is near 0, either the nonlinear absorber prevents the pendulum to reach high amplitude of oscillation, or it allows the pendulum to vibrate with acceptable amplitude. However, this is function of the parameters of the absorber. This behavior could be improved with other parameters.

4.3 The general case

In the general case, as in the vertical excitation case, it is impossible to see the maximum amplitude of equilibrium points of the system. There are some equilibrium points that are on the stable branch with high amplitudes that is split into two branches. As in the previous section, for low and high values of frequency, the behavior of the system with nonlinear absorber is similar to the behavior of the reference system. For σ near 0, the same barrier avoids the system to reach high amplitude equilibrium points from low amplitude initial conditions.

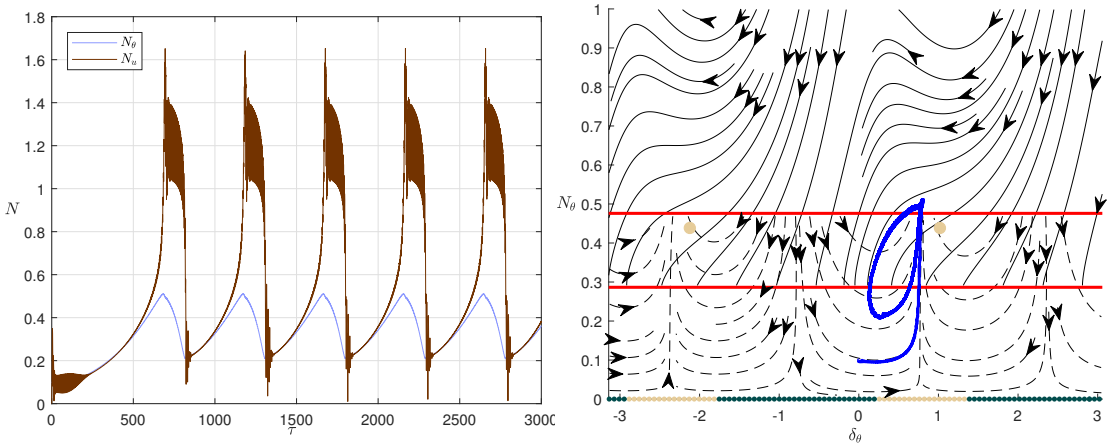

(a) Amplitude vs. time

(b) Phase portrait $(\delta_\theta, N_\theta)$.

Figure 22: Numerical integration illustrating SMR phenomenon (excitation: $y_2 = 0.25$, $\sigma = 0.5$, initial conditions: $\Theta(0) = 0.1$, $U(0) = 0$).

5 Conclusion

The nonlinear passive control problem of a single-degree-of-freedom pendulum subjected to base and external excitations is studied. It is assumed that the excitations are periodic which their frequencies vary in vicinity of the pendulum frequency. The nondimensionalised form of system equations are complexified and are treated by a time multiple scale method. All characteristic points of the system and their stabilities for the pendulum without and with coupled nonlinear absorber are revealed.

It is seen that lateral base excitation (horizontal) has the same effects as of horizontal external excitation. The system can present periodic or strongly modulated responses which by proper design can keep amplitude of variations of the pendulum in a given threshold.The latter can last for a while before the system gets attracted by a periodic response. Poincaré maps of the system are traced and detected numerical equilibrium points are compared with analytically predicted ones. It is shown that the duration of the strongly modulated responses depends on the initial conditions.

The system (without coupled nonlinear absorber) under parametric excitation (vertical) can possess stable equilibrium points with very high amplitudes. We showed that the absorber can create a barrier preventing the system to reach these equilibrium points. The case with combination of horizontal and vertical base excitation is more complex, but the phenomenon of barrier also exists.

Developed techniques provide design tools for tuning parameters of the nonlinear absorber to control the pendulum vibrations due to external and base excitations.

Funding The authors would like to thank “La Region Auvergne–Rhone–Alpes” for supporting this work in the frame of the CALIPSO Project (CALIPSO Contract 17 010971 01 - 15713).

Compliance with ethical standard

Conflict of interest The authors declare no conflict of interest.

References

[1] Hermann Frahm. "Device for damping vibrations of bodies." Pat. US Patent 989,958. 1911 (cit. on p. 1).

[2] J. P. Den Hartog. *Mechanical vibrations*. New York, 1956 (cit. on p. 1).

[3] Hiroshi Matsuhisa and Masashi Yasuda. "Dynamic vibration absorber for pendulum type structure". Pat. US Patent 5,460,099. 1995 (cit. on p. 1).

[4] Hiroshi Matsuhisa, Rongrong Gu, Yongjing Wang, Osamu Nishihara, and Susumu Sato. "Vibration Control of a Ropeway Carrier by Passive Dynamic Vibration Absorbers". *JSME international journal. Ser. C, Dynamics, control, robotics, design and manufacturing* 38.4 (1995), pp. 657–662. DOI: 10.1299/jsmec1993.38.657 (cit. on p. 1).

[5] L. D. Viet and Youngjin Park. "Vibration control of the axisymmetric spherical pendulum by dynamic vibration absorber moving in radial direction". *Journal of Mechanical Science and Technology* 25.7 (2011), pp. 1703–1709. DOI: 10.1007/s12206-011-0418-8 (cit. on p. 1).

[6] Robert E. Roberson. "Synthesis of a nonlinear dynamic vibration absorber". *Journal of the Franklin Institute* 254.3 (1952), pp. 205–220. DOI: 10.1016/0016-0032(52)90457-2 (cit. on p. 1).

[7] Eugene Sevin. "On the Parametric Excitation of Pendulum-Type Vibration Absorber". *Journal of Applied Mechanics* 28.3 (1961), p. 330. DOI: 10.1115/1.3641707 (cit. on pp. 1 sq.).

[8] W. J. Carter and F. C. Liu. "Steady-State Behavior of Nonlinear Dynamic Vibration Absorber". *Journal of Applied Mechanics* 28.1 (1961), p. 67. DOI: 10.1115/1.3640468 (cit. on p. 1).

[9] R. A. Struble and J. H. Heinbockel. "Resonant Oscillations of a Beam-Pendulum System". *Journal of Applied Mechanics* 30.2 (1963), p. 181. DOI: 10.1115/1.3636509 (cit. on p. 1).

[10] D. M. Egle. "An Investigation of an Impact Vibration Absorber". *Journal of Engineering for Industry* 89.4 (1967), p. 653. DOI: 10.1115/1.3610127 (cit. on p. 1).

[11] R. S. Haxton and A. D. S. Barr. "The Autoparametric Vibration Absorber". *Journal of Engineering for Industry* 94.1 (1972), p. 119. DOI: 10.1115/1.3428100 (cit. on p. 1).

[12] Izumo Yamakawa, Sadahiko Takeda, and Hiroyuki Kojima. "Behavior of a New Type Dynamic Vibration Absorber Consisting of Three Permanent Magnets". *Bulletin of JSME* 20.146 (1977), pp. 947–954. DOI: 10.1299/jsme1958.20.947 (cit. on p. 1).

[13] R. Riganti. "Extinction of predominantly subharmonic oscillations in a non linear dynamic damper with two degrees of freedom". *Mechanics Research Communications* 5.3 (1978), pp. 113–119. DOI: 10.1016/0093-6413(78)90041-1 (cit. on p. 1).

[14] J.B. Hunt and J.-C. Nissen. "The broadband dynamic vibration absorber". *Journal of Sound and Vibration* 83.4 (1982), pp. 573–578. DOI: 10.1016/S0022-460X(82)80108-9 (cit. on p. 1).

[15] H. Kojima and H. Saito. "Forced vibrations of a beam with a non-linear dynamic vibration absorber". *Journal of Sound and Vibration* 88.4 (1983), pp. 559–568. DOI: 10.1016/0022-460X(83)90657-0 (cit. on p. 1).

[16] Jinsiang Shaw, Steven W. Shaw, and Alan G. Haddow. "On the response of the non-linear vibration absorber". *International Journal of Non-Linear Mechanics* 24.4 (1989), pp. 281–293. DOI: 10.1016/0020-7462(89)90046-2 (cit. on p. 1).

[17] Y. Song, H. Sato, Y. Iwata, and T. Komatsuzaki. "The response of a dynamic vibration absorber system with a parametrically excited pendulum". *Journal of Sound and Vibration* 259.4 (2003), pp. 747–759. DOI: 10.1006/jsvi.2002.5112 (cit. on pp. 1 sq.).

[18] G. Habib and G. Kerschen. "A principle of similarity for nonlinear vibration absorbers". *Physica D: Nonlinear Phenomena* 332 (2016), pp. 1–8. DOI: 10.1016/j.physd.2016.06.001 (cit. on p. 1).

[19] O. Gendelman, L. I. Manevitch, A. F. Vakakis, and R. M'Closkey. "Energy Pumping in Nonlinear Mechanical Oscillators: Part I-Dynamics of the Underlying Hamiltonian Systems". *Journal of Applied Mechanics* 68.1 (2001), p. 34. DOI: 10.1115/1.1345524 (cit. on p. 1).

[20] A. F. Vakakis and O. Gendelman. "Energy Pumping in Nonlinear Mechanical Oscillators: Part II. Resonance Capture". *Journal of Applied Mechanics* 68.1 (2001), p. 42. DOI: 10.1115/1.1345525 (cit. on p. 1).

[21] Sean A. Hubbard, D. Michael McFarland, Lawrence A. Bergman, and Alexander F. Vakakis. "Targeted Energy Transfer Between a Model Flexible Wing and Nonlinear Energy Sink". *Journal of Aircraft* 47.6 (2010), pp. 1918–1931. DOI: 10.2514/1.C001012 (cit. on p. 1).

[22] C.-H. Lamarque, O. V. Gendelman, A. Ture Savadkoohi, and E. Etcheverria. "Targeted energy transfer in mechanical systems by means of non-smooth nonlinear energy sink". *Acta Mechanica* 221.1-2 (2011), pp. 175–200. DOI: 10.1007/s00707-011-0492-0 (cit. on p. 1).

[23] Mohammad A. AL-Shudeifat. "Highly efficient nonlinear energy sink". *Nonlinear Dynamics* 76.4 (2014), pp. 1905–1920. DOI: 10.1007/s11071-014-1256-x (cit. on p. 1).

[24] Etienne Gourc, Guilhem Michon, Sébastien Seguy, and Alain Berlioz. "Targeted Energy Transfer Under Harmonic Forcing With a Vibro-Impact Nonlinear Energy Sink: Analytical and Experimental Developments". *Journal of Vibration and Acoustics* 137.3 (2015). DOI: 10.1115/1.4029285 (cit. on p. 1).

[25] Gabriel Hurel, Alireza Ture Savadkoohi, and Claude-Henri Lamarque. "Nonlinear vibratory energy exchanges between a two degrees-of-freedom pendulum and a nonlinear absorber." *Journal of Engineering Mechanics* 145.8 (2019), p. 04019058. DOI: 10.1061/(ASCE)EM.1943-7889.0001620 (cit. on p. 1).

[26] Gabriel Hurel, Alireza Ture Savadkoohi, and Claude-Henri Lamarque. "Passive control of a two degrees-of-freedom pendulum by a non-smooth absorber". *Nonlinear Dynamics* 98.4 (2019), pp. 3025–3036. DOI: 10.1007/s11071-019-04891-0 (cit. on p. 1).

[27] R.W. Leven and B.P. Koch. "Chaotic behaviour of a parametrically excited damped pendulum". *Physics Letters A* 86.2 (1981), pp. 71–74. DOI: 10.1016/0375-9601(81)90167-5 (cit. on p. 1).

[28] J. C. Sartorelli and W. Lacarbonara. "Parametric resonances in a base-excited double pendulum". *Nonlinear Dynamics* 69.4 (2012), pp. 1679–1692. DOI: 10.1007/s11071-012-0378-2 (cit. on p. 1).

[29] John Miles. "Parametric excitation of an internally resonant double pendulum". *ZAMP Zeitschrift for angewandte Mathematik und Physik* 36.3 (1985), pp. 337–345. DOI: 10.1007/BF00944628 (cit. on p. 1).

[30] Leonid I. Manevitch, Valeri V. Smirnov, and Francesco Romeo. "Non-stationary resonance dynamics of the harmonically forced pendulum". *arXiv:1604.06670 [nlin]* (2016) (cit. on p. 1).

[31] Margarita Kovaleva, Leonid Manevitch, and Francesco Romeo. "Stationary and non-stationary oscillatory dynamics of the parametric pendulum". *Communications in Nonlinear Science and Numerical Simulation* 76 (2019), pp. 1–11. DOI: 10.1016/j.cnsns.2019.02.016 (cit. on p. 1).

[32] L. I. Manevitch and V. V. Smirnov. "Limiting phase trajectories and the origin of energy localization in nonlinear oscillatory chains". *Physical Review E* 82.3 (2010). DOI: 10.1103/PhysRevE.82.036602 (cit. on p. 1).

[33] Ali Hasan Nayfeh and Dean T. Mook. *Nonlinear oscillations*. Wiley classics library ed. Wiley classics library. New York, 1995 (cit. on p. 1).

[34] J Awrejcewicz and R Starosta. "Resonances in a kinematically driven nonlinear system-Asymptotic analysis". *Journal| MESA* 1.1 (2010), pp. 81–90 (cit. on p. 1).

[35] Jan Awrejcewicz, Roman Starosta, and Grażyna Sypniewska-Kamińska. "Asymptotic Analysis of Resonances in Nonlinear Vibrations of the 3-dof Pendulum". *Differential Equations and Dynamical Systems* 21.1-2 (2013), pp. 123–140. DOI: 10.1007/s12591-012-0129-3 (cit. on p. 1).

[36] Jan Awrejcewicz, Roman Starosta, and Grażyna Sypniewska-Kamińska. "Stationary and Transient Resonant Response of a Spring Pendulum". *Procedia IUTAM* 19 (2016), pp. 201–208. DOI: 10.1016/j.piutam.2016.03.026 (cit. on p. 1).

[37] Roman Starosta, Grażyna Sypniewska-Kamińska, and Jan Awrejcewicz. "Asymptotic analysis of kinematically excited dynamical systems near resonances". *Nonlinear Dynamics* 68.4 (2012), pp. 459–469. DOI: 10.1007/s11071-011-0229-6 (cit. on p. 1).

[38] K.M. Jackson, J. Joseph, and S.J. Wyard. "A mathematical model of arm swing during human locomotion". *Journal of Biomechanics* 11.6-7 (1978), pp. 277–289. DOI: 10.1016/0021-9290(78)90061-1 (cit. on p. 2).

[39] A. Ture Savadkoohi, C.-H. Lamarque, and C. Goossaert. "Nonlinear passive tremor control of human arm". *Mechanical Systems and Signal Processing* 146 (2021), p. 107041. DOI: 10.1016/j.ymssp.2020.107041 (cit. on p. 2).

[40] Jan Awrejcewicz and Grzegorz Kudra. "The piston — Connecting rod — Crankshaft System as a triple physical pendulum with impacts". *International Journal of Bifurcation and Chaos* 15.07 (2005), pp. 2207–2226. DOI: 10.1142/S0218127405013290 (cit. on p. 2).

[41] J Awrejcewicz, G Kudra, and C-H Lamarque. "Dynamics investigation of three coupled rods with a horizontal barrier". *Meccanica* 38.6 (2003), pp. 687–698 (cit. on p. 2).

[42] Jan Awrejcewicz, Grzegorz Kudra, and Claude-Henri Lamarque. "Investigation of triple pendulum with impacts using fundamental solution matrices". *International Journal of Bifurcation and Chaos* 14.12 (2004), pp. 4191–4213. DOI: 10.1142/S0218127404011818 (cit. on p. 2).

[43] Takashi Ikeda. "Nonlinear Responses of Dual-Pendulum Dynamic Absorbers". *Journal of Computational and Nonlinear Dynamics* 6.1 (2011). DOI: 10.1115/1.4002385 (cit. on p. 2).

[44] L. I. Manevitch. "The Description of Localized Normal Modes in a Chain of Nonlinear Coupled Oscillators Using Complex Variables". *Nonlinear Dynamics* 25.1 (2001), pp. 95–109. DOI: 10.1023/A:1012994430793 (cit. on pp. 4, 9).

[45] K. O. Friedrichs and J. J. Stoker. "Forced vibrations of systems with nonlinear restoring force". *Quarterly of Applied Mathematics* 1.2 (1943), pp. 97–115 (cit. on p. 5).

[46] A. Ture Savadkoohi, C.-H. Lamarque, M. Weiss, B. Vaurigaud, and S. Charlemagne. "Analysis of the 1:1 resonant energy exchanges between coupled oscillators with rheologies". *Nonlinear Dynamics* 86.4 (2016), pp. 2145–2159. DOI: 10.1007/s11071-016-2792-3 (cit. on p. 11).

[47] Y. Starosvetsky and O.V. Gendelman. "Strongly modulated response in forced 2DOF oscillatory system with essential mass and potential asymmetry". *Physica D: Nonlinear Phenomena* 237.13 (2008), pp. 1719–1733. DOI: 10.1016/j.physd.2008.01.019 (cit. on p. 16).